INTERNATIONAL JOURNAL OF ENERGY
DOI: 10.46300/91010.2021.15.16 Volume 15, 2021

Supervisor Control for a Stand–Alone Hybrid Generation System Using Fuel Cell and Photovoltaic Energy

Mourad Tiar, Achour Betka, Ridha Cheikh
LGEB Laboratory, Electrical Engineering Department
University Mhamed KHeider
Biskra, Algeria
Email: tiarmourad@yahoo.com,
betkaachour@gmail.com, cheikh_red@yahoo.fr

Said Drid
LSPIE Laboratory, Electrical Engineering Department
Batna University
Batna ,Algeria
Email: s_drid@yahoo.fr

Abstract – this paper discusses a comprehensive supervisor control for a hybrid system that comprises the photovoltaic generation , hydrogen system (Fuel cell ,Electrolyse) and an ac load is developed in this paper. The objectives of the supervisor control are, primarily, to satisfy the load power demand and, second, allows to store the gas through the electrolyser. For these purposes, the supervisor controller determines the operation mode online of the solar generation subsystem , switching from power regulation to maximum power conversion . Decision criteria for the supervisor based on measurable system variables are presented (voltages, and currents) . Finally, the performance of the supervisor controller is extensively assessed through computer simulation using a comprehensive nonlinear model .

Keywords – Power Control , Photovoltaic, fuel cell, Electrolyzer .

List of Symbols:

I_{cc} : Short-circuit current (A)

I_o : Current of opposite saturation of the diode (A)

R_s: photovoltaic panel (Ω)

r_s: Series resistance of the generator (Ω)

V_{th}: Thermal voltage (V)

V_{op}: Optimal voltage (V)

I_{op}: Optimal current (A)

V_{oc} : Open-circuit voltage (V)

N_S : Series panels number

N_P : parallel branches number

T: temperature (°K)

E : Irradiance level

E_{oc} : Full cell open-circuit (V)

V_{cell} : Full cell voltage (V)

V_{bus}: DC bus voltage (V)

I_{pv} : current generated by the PV array (A)

I_L : load current (A)

I_{fuel} : fuel cell current injected on the dc bus (A).

I_{elc} : electrolyser current (A)

α_{mppt} : Duty cycle

α_{fuel} : Duty cycle

α_{elc} : Duty cycle

I. Introduction:

The use of renewable resources, outside the main hydraulic [1] , is generally limited to isolated sites where the cost of renewable systems become competitive with other forms of electricity generation because of the delivery of very expensive electricity.

There are many isolated sites in the world, fuelled by autonomous systems of electricity generation. These generators use local renewable sources.

There are solar panels, wind turbines and micro turbines. Electricity from renewable sources is intermittent, dependent on climatic conditions. These generators are coupled to a renewable storage system providing continuous availability of energy.

Usually the storage is provided by battery. These systems, called PV Battery are currently the most widely used solutions. The battery have very good yields of the order of 80-85%, and a very competitive price, if we considers the lead technology. But its disadvantages are numerous and limited storage.

To improve PV-Battery while maintaining their quality and respect for the environment, an idea appeared in the 90s, is to use hydrogen to store energy in the long term. Indeed, the gas can be produced by an electrolyser, stored without significant loss regardless of the duration of storage, and then converted into electricity in a fuel cell. These systems, called Solar - Hydrogen or PV-Hydrogen has many advantages: no moving parts and the electrolyser and fuel cells produce very little noise. In addition, these components are expected high reliability, low operating constraints and limited maintenance. However, the use of hydrogen as energy storage increases the complexity of installations. Much research has been conducted on the Solar-Hydrogen systems. These studies have met with the low maturity of electrolysers and fuel cells.

The development of hydrogen technologies has been very important during the past decade. Progress can be considered high performance « system for hydrogen storage ».

II.SYSTEM DESCRIPTION:

In our system Studied Figure (1), the field photovoltaic (PV) directly supplies the user. The solar excess is stored chemical form [2] an electrolyser (EL) separates the water into hydrogen and oxygen. The gas is stored without loss regardless of the storage time. When the solar field can not provide all of the electricity demand, the fuel cell is connected. It regenerates the electricity stored in recombinant hydrogen and oxygen. The fuel cell (FC) produces pure water that is stored to supply the electrolyser [6].The topology of the hybrid system under consideration in this paper is depicted in Fig (1) the solar array comprises several PV panels connected to the DC bus via a boost DC/DC converter. The converter permits to track the available maximum power [3].

The boost chopper related to the PEM fuel cell, permits through the control of the dc link voltage to collect the energy generated by both the PV modules and the fuel cell in order to feed the load, and the buck chopper connected to the electrolyser . So the control of the single-phase inverter ensures a pure sine wave with a low total distortion factor (THD).

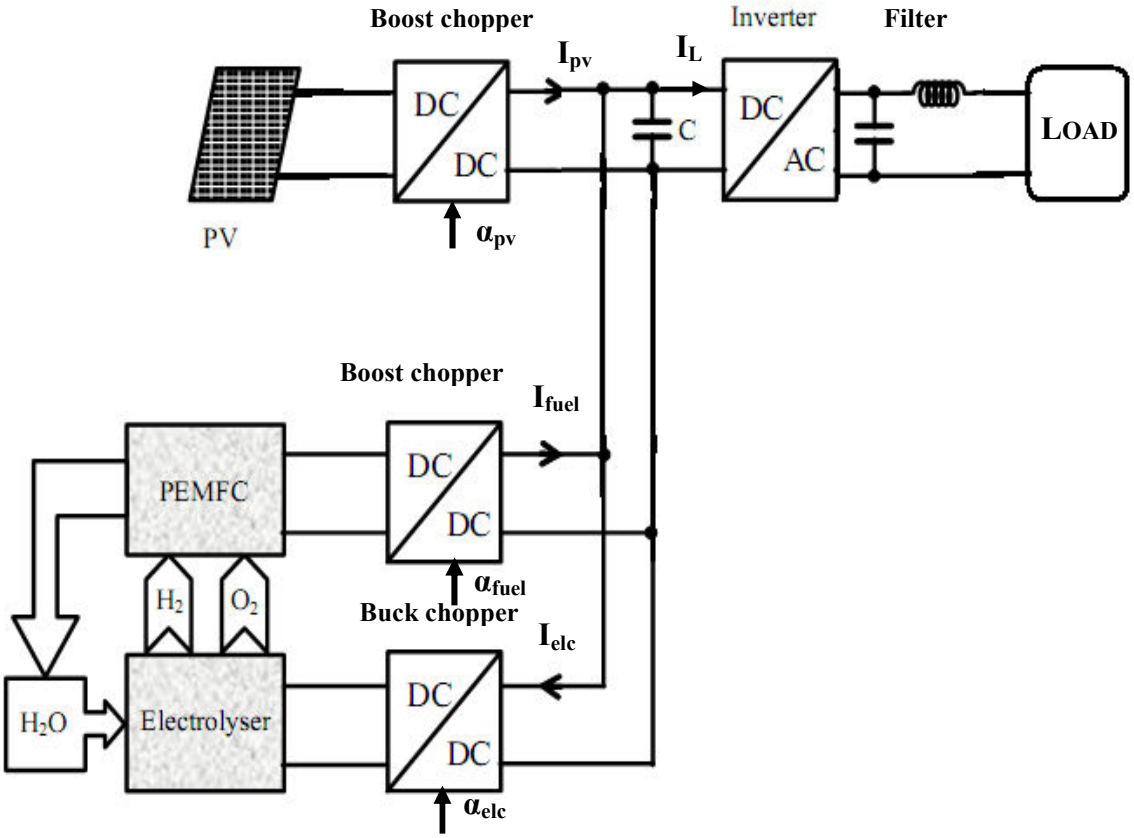

Fig(1):Hybrid generation system

III.SYSTEM MODELLING:

A. PV Array model:

The used 4.2 Kwp PV generator is constituted by 4 parallel strings of 34 modules each; where the (I-V) characteristic is modeled by the following nonlinear implicit equation [4]:

$$I = I_{cc} - I_o\left[\exp\left(\frac{V + R_s I}{V_{th}}\right) - 1\right] \quad (1)$$

Where, the thermal voltage Vth and the saturation current Io are identified by:

$$V_{th} = \frac{V_{op} + R_s I_{op} - V_{oc}}{\log\left(1 - \frac{I_{op}}{I_{cc}}\right)} \quad (2)$$

$$I_o = \left(I_{cc} - I_{op}\right)\exp\left[-\frac{(V_{op} + R_s I)}{V_{th}}\right] \quad (3)$$

For other irradiance and temperature levels, we can use the following laws:

$$\Delta T = T - T_{ref} \quad (4)$$

$$\Delta I = \alpha\left(\frac{E}{E_{ref}}\right)\Delta T + \left(\frac{E}{E_{ref}} - 1\right)I_{ccref} \quad (5)$$

$$\Delta V = -\beta \Delta T - r_s \Delta I \quad (6)$$

With:

$$r_s=(N_S/N_P).R_S \quad (7)$$

Thus the new values of current and voltage are in the form:

$$V=V_{ref} + \Delta V \quad (8)$$

$$I=I_{ref} + \Delta I \quad (9)$$

The coefficient of variation of the current and voltage are respectively a functions of temperature (α = 0.06 %/ °c), (β = 0.4 % /°c) .

B. Modelling of the hydrogen system :

The model used in this article is from the empirical point of view approach. This model enables to simulate both fuel cells and electrolyser (V-j) curves (cell voltage versus current density) in typical conditions [5].

The low temperature PEM fuel cell stack used in this paper is constituted of 60 cells connected in series, with 4kW rated power. The electrical a model given in equation (10), inspired from [2], permits a good matching of the experimental curve:

$$V_{cell}(J) = E_{oc} + \frac{b}{\ln\left(\frac{J}{J_d e^2}\right)} + \left(\frac{b}{4J_d} - \Delta\right) J \quad (10)$$

Where the four fitting parameters (Eoc, Jd, b and Δ) depend on both the cell temperature T and the oxygen partial pressure PO2. Each parameter is dissociated on three components, and can be solved through the following equation: [7]

$$\begin{bmatrix} E_{oc} \\ J_d \\ b \\ \Delta \end{bmatrix} = \begin{bmatrix} E_{oc1} & E_{oc2} & E_{oc3} \\ J_{d1} & J_{d2} & J_{d3} \\ b_1 & b_2 & b_3 \\ \Delta_1 & \Delta_2 & \Delta_3 \end{bmatrix} \cdot \begin{bmatrix} 1 \\ T \\ T.\ln(P_{o2}) \end{bmatrix} \quad (11)$$

In this article, the data presented in Tables (1) and (2) respectively according to the electrolyser and fuel cell are retained.

Fuel cell			
Jd	- 0,868	- 1,762e-3	4,9e-4
Eoc	0,796	4,661e-3	- 3,22e-4
b	- 1,926	2,616e-2	- 1,489e-3
Δ	3,892	- 7,447e-3	- 2,696e-4

TABLE (1): ELECTRICAL MODEL CONSTANTS OF THE PEM FUEL CELL

Électrolyser			
Jd	0,355	- 1,078e-3	5,232e-5
E	1,025	1,24e-3	- 1,05e-4
b	- 6,125	1,57e-2	- 3,245e-4
Δ	- 1,819	4,83e-3	- 1,248e-4

TABLE (2): ELECTRICAL MODEL CONSTANTS OF THE ELECTROLYSER.

C. *Average state-space models of the static converters:*

The main purpose of modeling the different used static converters by average expressions is to expose their dynamic behaviors by continuous canonical forms, since these switched systems commutate between more than a continuous states; and consequently, the development of the control laws is difficult [7].

- Average dynamic model of the boost chopper:

In figure (2) is depicted the conventional scheme of a boost chopper, fed by a dc voltage source Ve. The average state-space model given by equation (12) is derived by computing the average dynamic state x, and where the duty cycle α is considered as a parameter [8]:

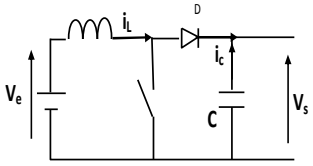

Fig. (2): Boost chopper scheme

$$\begin{cases} \dot{x}_1 = -\dfrac{1-\alpha}{L} x_2 + \dfrac{1}{L} u \\ \dot{x}_2 = \dfrac{1-\alpha}{c} x_1 + \dfrac{1}{RC} x_2 \end{cases} \quad (12)$$

Where:

$x = [i_L, V_C]$; u: V_e

- Average dynamic model of the buck chopper:

In figure (3) is depicted the conventional scheme of a buck chopper [9] .

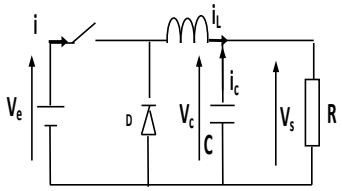

Fig. (3): Buck chopper scheme

$$\begin{cases} \dot{x}_1 = -\frac{1}{L}x_2 + \frac{\alpha}{L}u \\ \dot{x}_2 = \frac{1}{c}x_1 - \frac{1}{RC}x_2 \end{cases} \quad (13)$$

$$y = x_2$$

where

$x=[i_L, v_c]$; $u=V_e$.

IV. OPERATION STRATEGY AND SUPERVISOR CONTROL:

A. *General Description of the Supervisor Control Policy:*

There are many isolated sites in the world, fueled by autonomous systems of electricity generation. These generators use local renewable sources. There are solar panels, wind turbines and micro-turbines. Electricity come from renewable sources is intermittent, dependent on climatic conditions. These renewable generators are coupled to a hydrogen storage system ensuring continuous availability of energy.

A comprehensive supervisor control algorithm is essential to efficiently manage the operation of the generation subsystems according to those modes.

The supervisor control commands the solar subsystem either regulating power or tracking the PV maximum power conversion point (Mode 1 and Mode 2 or Mode 3, respectively)..

This surveillance adequate for proper functioning of sub-systems of renewable energy production is done in three modes.

B. *Description of operating modes:*

The energy management of the various sources is provided by a supervisor. This determines the operating mode following three cases proposed. These operating modes are possible to determine system capacity to satisfy the total demand (load demand) . It should be noted that the fuel cell and electrolyser are operated in complementarily. On figure (4) is shown the description of the operating modes available.

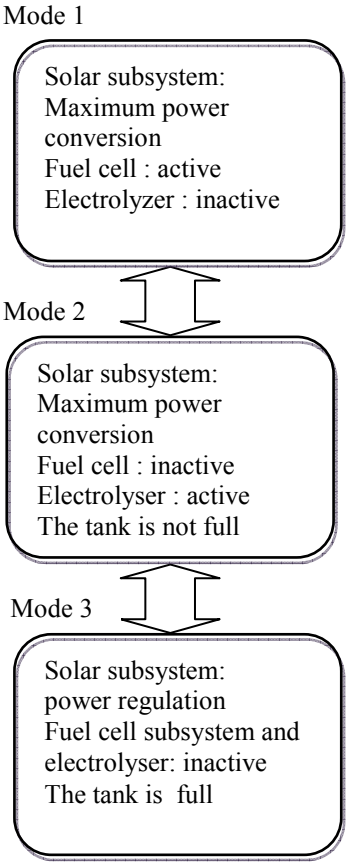

Fig (4) : Schematic description of the operation modes.

- *MODE 1 (MPPT AND AUXILIARY SOURCE):*

In this mode, the PV generator provides maximum power , MPPT (tracking the maximum power conversion point) ,this power is insufficient to satisfy the load demand, and the fuel cell completed the power demanded by the load. When the power supplied by the generator exceeds the total power demanded by the load, the supervisor sets the system to mode 2.

- *MODE 2 (GAS STORAGE):*

In this mode, the tank is not full. The excess energy produced by the photovoltaic generator is stored as a gas through the electrolyser. this Mode is maintained until the volume of gas tank does not reach the maximum threshold . Beyond this limit, the supervisor switches the system to mode 3.

- *MODE 3 (POWER REGULATION):*

In this mode, the tank is full, the photovoltaic generator provides necessary power (power regulation) to satisfy the demand of the load, however the hydrogen subsystem is inactive. When the maximum power of the PV generator does not satisfy this request, the supervisor between the system in mode 1.

V. *SOLAR SUBSYSTEM OPERATION :*

The supervisor control commands the solar subsystem either regulating power or tracking the PV maximum power conversion point (Mode 1 and mode 2 or Mode 3, respectively) ; In Mode 1, the objective of the fuel cell is to complement the solar generation to satisfy the total power demand.

such that the power of the fuel cell is:

$$P_{fuel} = P_{ch} - P_{pv\max} \quad (14)$$

Therefore, the reference for the PV generated power results:

$$P_{sref} = V_{bus} I_{pvm} \quad (15)$$

In Fig. 4(a), the generated current of a PV panel array with fixed insolation and temperature (shown in the solid line) are presented along with the PV power reference P_{sref} (dashed line) and the locus of maximum power conversion for different degrees of insolation (dashed-dotted line). In correspondence, Fig. 4(b) depicts the power–voltage plane, the PV generated power (solid line), the PV power reference (dashed line), and the locus of maximum power conversion (dashed-dotted line) for different atmospheric conditions. The intersection of the latter with the curve in solid line (point C) corresponds to the maximum power operation point (MPOP) of the PV array for those particular values of insolation and temperature

In these figures, it can be appreciated that two operation points exist, capable of generating the reference power (points A and B); therefore, the operation on the left-hand side of the MPOP (point A side) would be quite restrictive provided that the power regulation would be significantly bounded. Conversely, operating in the right-hand side of the MPOP (point B side) allows a broad range of power regulation; therefore, this side has been chosen for operation. A reliable criterion to decide when to switch from PV maximum power generation (Mode 1 or Mode 2) to power regulation (Mode 3) must be deduced.

Then, the first step is to establish the position of the MPOP (point C in Fig. 4) by zeroing the derivative of the power [14] .

$$\frac{\partial P_{pv}}{\partial V_{pv}} = 0 \quad (16)$$

Where :

$$\frac{\partial \left(i_{pv} V_{pv} \right)}{\partial V_{pv}} = 0 \quad (17)$$

We deduce the condition of the incremental conductance [10]:

$$\frac{\partial i_{pv}}{\partial V_{pv}} V_{pv} + i_{pv} = 0 \quad (18)$$

From equation (4-3), the following expression is derived:

$$P_f = -\frac{\partial i_{pv}}{\partial V_{pv}} V_{pv}^2 \quad (19)$$

Where :

$$P_f \cong -\frac{\Delta i_{pv}}{\Delta V_{pv}} V_{pv}^2 \quad (20)$$

Evidently, (20) evaluated at the MPOP voltage provides the maximum solar power. However, when (20) is computed for other values of V_{pv} , it results not in actual power but in fictitious power P_f . Such fictitious power can be directly utilized to determine the mode of operation of the solar subsystem, for example, constant insolation and the subsystem regulating power (Mode 3) on a point situated on the right-hand side of the MPOP. It can be appreciated in Fig. 4(a) that in this side, the (i_{pv}-v_{pv}) curve presents a highly negative slope.

Therefore, for any right-hand side operation, point Pf is greater than the power corresponding to the MPOP and, obviously, greater than the actual power at the present point of operation Psref . Then, if te operation point approached the MPOP, the actual PV power would also approach the fictitious power.

The supervisor control can take advantage of this singularity to select the mode of operation according to figure(5) .

If $P_f \prec P_{sref}$ ⇨ Mode 1:
- PV System: Maximum Power Conversion
- The fuel cell (source auxiliary) : active
- The electrolyser: inactive

If { $P_f \prec P_{sref}$; The gas tank is not full } ⇨ Mode 2 :
- PV System: Power Regulation
- $P_{sref} = V_{bus} I_{pvm}$
- The fuel cell (source auxiliary) and the electrolyzer : inactives

If { $P_f \geq P_{sref}$; The gas tank is full } ⇨ Mode 3 :
- PV System: Maximum Power Conversion
- The fuel cell (source auxiliary) : inactive
- The electrolyser : active.

Fig (5): Operating principle of the Intelligent supervisor

VI. SIMULATION RESULTS:

Computer simulations have been conducted for the nonlinear model of the system PV-Hydrogen to assess the performance of the supervisor control.

In Figures (6) and (7) are respectively represented the irradiance levels, which have an average of 800 W / m² and the load profile however these curves represent the input system.

In Figures (8), (9) and (10) are shown the powers provided / absorbed by the various subsystems (GPV, fuel cell and electrolyser), while specifications (11) and (12) respectively describe the conditions and the switching of the various operating modes.

From these graphs, the following conclusions are extracted:

- From (0 to 0.2s), the load demand is 1 .5 kw, while the PV generator has been designed for a power greater (about 2.2 kw), which corresponds to the level of irradiance

E = 600 w / m² see table (3) and the gas tank is full while the PV generator satisfied this demand see figure (8) , therefore the system operated in mode 3 (see Figure (12)), the fuel cell and electrolyser are inactive (see Figure (9) and (10)).

- From (0.2 to 0.4s): the load demand increases to 500 W, and the level of irradiance changed from 600 to 800 w / m². Given that the tank is supposed to full, the system always operates in mode 3 (figure (12) and GPV delivers the power of the load (2 kw) figure (8).

- From (0.4 to 0.6s): the load demand peak is observed (equal to 7 kilowatts), while the irradiance level increased at 1000w / m². at this condition, the GPV is unable to satisfy load demand and the system switches to mode 1 (Fig. (12)), where GPV operated of the MPPT, it's delivered about 4.1 kilowatts see table (3), however the fuel cell (auxiliary source) delivered about 2.8kW to satisfy the demand load (Fig. (9)).

- From (0.6 to 0.8s) the load demand is lowered at 2 kw, the PV generator covers this power, the supervisor control is switched anew to Mode 3 (see figure (12)).

- From (0.8 to 1.2s) : the storage gas tanks (H_2, O_2) are assumed not full. the irradiance level dates back in repeated sequence (Fig. (6)) and the load power oscillates around 1.7 KW while the power of GPV is greater, the supervisor control is switched to mode 2 (see figure (12)) therefore the excess power produced by the PV generator is stored as of the gas through the electrolyser see fig (10).

- From (1.2 to 1.4s): the load power is again find at the peak value (7 kw). The system returns again in Mode 1 or the GPV operates in MPPT, and the active fuel cell delivers the excess power to satisfy load demand (see Figure (9)).

E(W/m²)	Vop(V)	Iop(A)	Pop(W)
1000	209,4	19,8	4146,12
800	206,4	15,46	3190,94
600	204,19	11,12	2271,5

TABLE (3): OPTIMAL CHARACTERISTIC OF PV FOR DIFFERENTS LEVELS IRRADIANCE .

The supervisor control determines the operation modes of the system PV- hydrogen Fig. (12) by processing the information presented in figure (11).It should be remarked that the control supervisor is inactive for mode 2. This practice is followed to put the solar system is operated in MPPT and therefore the excess energy produced by the photovoltaic generator is stored as a gas through the electrolyser .

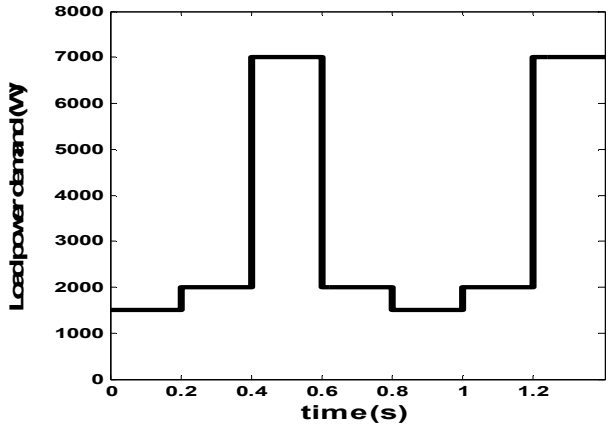

Fig (6): Irradiance level

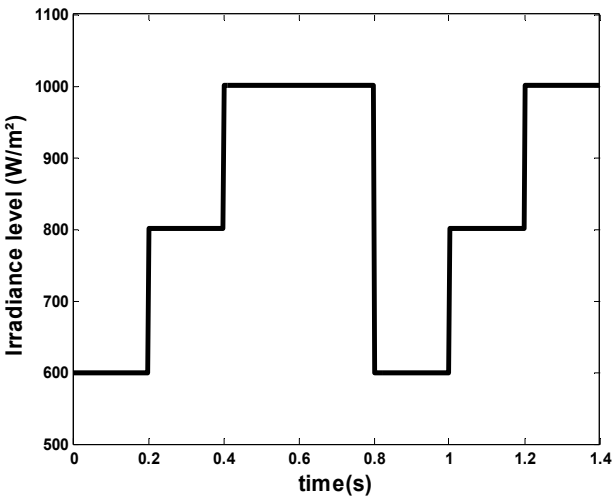

Fig(7) : Load Power demand

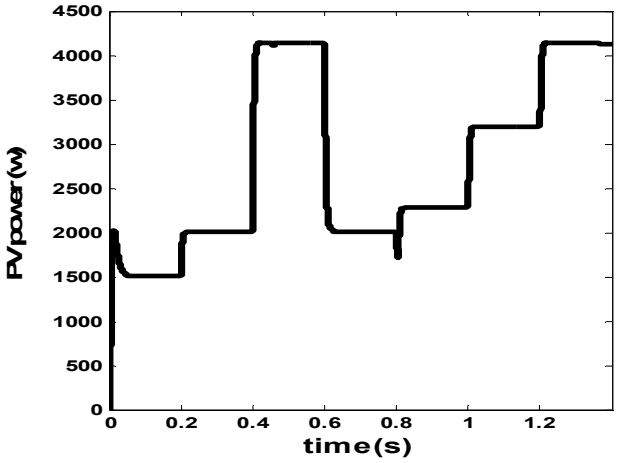

Fig (8) : PV power

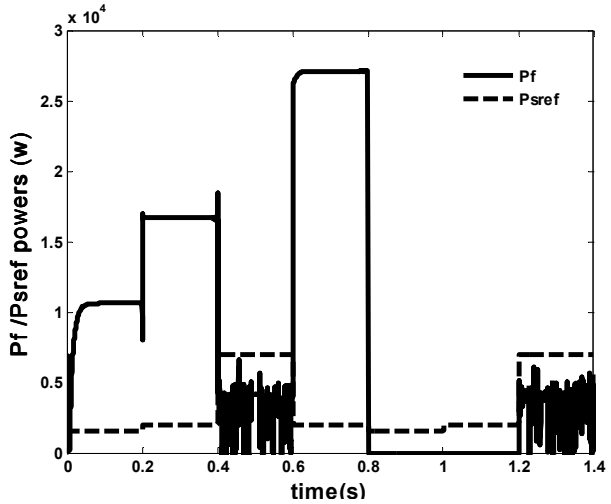

Fig (11) : Power fictitious and reference power

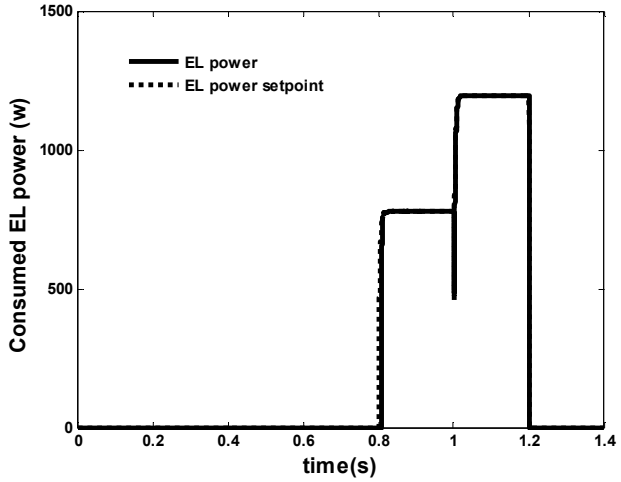

Fig (9) : Generated FC PEM power

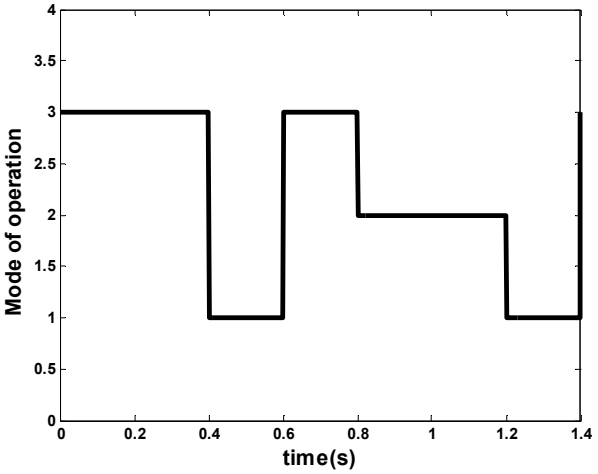

Fig (12) : mode of operation

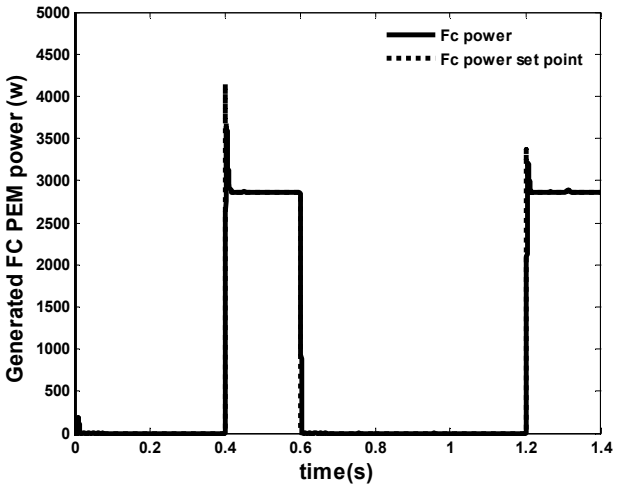

Fig(10) : Consumed electrolyser power

VII. CONCLUSION:

The performance of electric generation hybrid systems relies heavily on the existence of a custom-made supervisor control capable to efficiently administrate the diverse energy resources involved. The comprehensive supervisor system developed in this paper proved to be highly competent to manage and coordinate the operation of the system PV-Hydrogen . It provides a versatile decision framework to deter mine the operation mode .

One of its most attractive features is that reliable and unambiguous criteria based only on easily measurable solar system variables (voltages, and currents) have been proposed for the decision algorithms of the supervisor.

The proposed energy supervisor showed significant efficacy and this by flexible permutation of mode different of operation. the Robust control laws have been considered in this paper to fulfill the different control objectives (i.e., power regulation or maximum energy conversion is based in fuzzy logic) of the solar system [12], [13], [14] and the differents Regulators have demonstrated notable robustness vis-à-vis the change in operating mode and the load.

Finally, for the application considered in this paper, it was decided that the main generation role would be carried out by the solar subsystem would principal and the fuel cell subsystem play a complementary role .

REFERENCES :

[1] Nature, 1er November 2002, p.981.

[2] C. Dumbs, "Development of analysis tools for photovoltaic-diesel hybrid systems" , These de Ecole des Mines de Paris, 20/12/1999.

[3] B. S. Borowy and Z.M. Salameh, "Methodology for optimally sizing the combination of a battery bank and pv array in a wind/PV hybrid system," IEEE Trans. Energy Convers., vol. 11, no. 2, pp. 367–375, Jun. 1996.

[4] S. Arul Daniel and N. Ammasai Gounden, "A Novel Hybrid Isolated Generating System Based on PV Fed Inverter-Assisted Wind-Driven Induction Generators", IEEE Trans. Energy Conversion, vol. 19, no. 2, pp. 416-422, June 2004.

[5] S. Busquet, C.E. Hubert, J. Labbé, D. Mayer, R. Metkemei er, ''A New Approach to Empirical Electrical Modelling of a Fuel Cell, an Electrolyser Sources, 134, 2004, pp. 41-48.

[6] S. Busquet, R. Metkemeijer, P. Leroux, D. Mayer, "Stand-alone power system coupling a PV field and a fuel cell : Experimental results of the FC system", Proceedings of the France-Deutschland Fuel Cell Conference 2002, October 7th to 10th 2002, Forbach-Saarbrücken, pp. 85-92, 2002.

[7] Moussa, W.M. and J.E. Morris, 1990. Comparison between state-space averaging and PWM switch for switch mode power supply analysis. Proceedings of the 1990 IEEE Southern Tier Technical Conference, Apr. 25-25, IEEE Xplore Press, Binghamton, NY., pp: 15-21. DOI: 10.1109/STIER.1990.324626

[8] Mohd Saifuzam Jamri and 2Tan Chee Wei," Modeling and Control of a Photovoltaic Energy System Using the State-Space Averaging Technique", Department of Power Electronics and Drives, Faculty of Electrical Engineering, University Tekikal Malaysia Melaka, Malaysia, American Journal of Applied Sciences 7 (5): 682-691, 2010 ISSN 1546-923

[9] Ropp, M.E. and S. Gonzalez, 2009. Development of a MATLAB/simulink model of a single-phase grid- connected photovoltaic system. IEEE Trans. Energy Conver., 24: 195-202. DOI: 10.1109/TEC.2008.2003206

[10] K. H. Hussein, I. Muta, T. Hoshino, and M. Osakada, "Maximum photovoltaic power tracking: an algorithm for rapidly changing atmospheric conditions," Proc. Inst. Elect. Eng., Gen., Transm. Distrib., vol. 142, no. 1, 1995.

[11] S. Lalouni et Al. Fuzzy logic control of stand-alone photovoltaic system with battery storage. Journal of Power Sources (Elsevier) 193 (2009) 899–907.

[12] Ammasai Gounden,Sabitha Ann Peter, Himaja Nallandula and S. Krithiga, «Fuzzy logic controller with MPPT using linecommutated inverter for three-phase grid connected photo-voltaic systems», Renewable Energy, Vol: 34, N°:3, pp: 909-915, 2009.

[13] P.Siarry, F. Guely, «A genetic algorithm for optimizing Takagi- Sugeno fuzzy rule bases», Fuzzy sets system, vol: 99, N°: 1, pp: 37 – 47, 1998.

[14] F. Valenciaga and F. Puleston, "Supervisor Control for Stand Alone Hybrid Generation System Using Wind and Photovoltaic Energy", IEEE Trans. Energy Conversion, vol. 20, no. 2, pp. 398- 405, June 2005.

- *INDEX*

AEG-40 module is the component of our photovoltaic generator. It consists of 35 square cells in monocrystalline silicon solar cell, where each side has 10 cm. This module has the following features provided by the manufacturer at 1000 W / m² 25 ° C:
Maximum Power (Pmax) = 38.4 w.
Short-circuit current (Icc) = 2.41 A.
Open-circuit voltage (Voc) = 22.4 V.
Optimum current (Iop) = 2.2 A.
Optimum voltage (Vop)= 17.45 V.
Series resistance (RS) = 0.45 Ω.
Coefficient of variation of the current as a function of the Temperature = 0.06% / ° c.
Variation voltage Coefficient depending to the Temperature = 0.4% / ° c.
Filter characteristics
L=5mH; C=100µF.
DC bus Capacitor
C=1000µF
Boost / Buck Converter self
L=5mH